IJE TRANSACTIONS C: Aspects Vol. 28, No. 9, (September 2015) 1351-1358

International Journal of Engineering

Journal Homepage: www.ije.ir

Dynamic Analysis of a Rotor Supported on Ball Bearings with Waviness and Centralizing Springs and Squeeze Film Dampers

S. Modaresahmadi*[a], M. Ghazavi [a], M. Sheikhzad Saravani [b]

[a]*Department of Mechanical Engineering, TarbiatModares University, Tehran, Iran*
[b]*Department of Mechanical Engineering, University of Wollongong,Wollongong,Australia*

P A P E R I N F O

Paper history:
Received 13 October 2014
Received in revised form 10 August 2015
Accepted 03 September 2015

Keywords:
Squeeze-film Damper
Waviness
Ball Bearing
Bifurcation

A B S T R A C T

Squeeze film dampers (SFDs) are often used in machines with high rotational speed to reduce non-periodic behavior by creating external damping. There are some structural parameters which are of great importance in designing these systems, such as oil film thickness and inner race mass of SFD. Moreover, there is a crucial parameter associated with manufacturing process, under the title of waviness. Geometric imperfections are often called waviness if its wavelength is much longer than Hertzian contact width. In this paper, a system of a flexible rotor and two ball bearings with squeeze film dampers and centralizing springs and also consideration of waviness has been modeled and solved by a numerical integration method to investigate the system dynamic response. Results show that by increasing the number of wave lobes, non-periodic and chaotic behavior increases. This reveals the importance of manufacturing accuracy and necessity of taking this term into account in simulations. Moreover, by changing the oil film thickness, it is revealed that there is an optimal value for this parameter to provide maximum damping. In addition, with increasing the inner race mass of SFD, the disc displacement amplitude increases. This reveals the importance of utilizing light materials in manufacturing the SFDs.

doi: *10.5829/idosi.ije.2015.28.09c.13*

1. INTRODUCTION

Dynamic analysis of rotor-bearing systems has become of great importance, by growing the demand for more accurate operation in high speeds. This was more about ball bearings rather than hydrodynamic bearings, due to the instability and failure of the latter at higher speeds [1].

As ball bearings have little damping, rotors are often mounted on ball bearings with squeeze film dampers (SFD) to reduce the vibrations. SFDs are widely used in aircraft gas turbine engines to stabilize and reduce vibration [2]. Many researches in the field of nonlinear behavior of rotors mounted on SFDs have been carried out. Inayat Hussain [2, 3] has investigated the effects of various structural parameters on the rotor response, through bifurcation diagrams, for the system of a rotor mounted on SFDs, either with retaining springs or without them. He changed non-dimensional parameters of bearings, gravity and weight ratio and applied a numerical integration method to investigate the dynamic behavior of the systems and the range of period-2, period-4 and chaotic responses of the systems. Also, Squeeze- film dampers with rigid rotor was investigated in literature [4]. In addition, the effect of fluid inertia on the response of a flexible rotor system and pre-loaded SFD has been investigated by the San Andres, Vance [5]. Qin et al. [6] showed the effects of elastic support on the response of bearings and film forces in Jacobs et al. [7] worked on the foundation of a lubricant film in a deep groove ball bearing and observing its effect on the dynamics of bearing. In this paper, ball bearings with lubricant film are modeled by springs and dampers in the same way as is reported [6]. Also, they introduced new test rig which gave them the opportunity to test

*Corresponding Author's Email: Sina.modares@modares.ac.ir (S. Modares Ahmadi)

Please cite this article as: S. Modaresahmadi, M. Ghazavi, M. Sheikhzad Saravani, Dynamic Analysis of a Rotor Supported on Ball Bearings with Waviness and Centralizing Springs and Squeeze Film Dampers, International Journal of Engineering (IJE), TRANSACTIONS C: Aspects Vol. 28, No. 9, (September 2015) 1351-1358

variety of ball bearings in the same working condition.

Also, several researches have been carried out to enhance the SFD performance. Hahn et al. [8] presented a new model of the SFD in which an outer race was elastically attached to a rigid frame. They showed that the improved SFD is useful in the prevention of bistable, sub-synchronous and non- synchronous responses. Zhou et al. [9] presented a dynamic model of a rotor with SFD which has two clearances and investigated the behavior of the system by means of a numerical integration method. The SFD with two clearances is actually a combination of two SFDs separated by a race. The SFD with two clearances is called a dual clearance squeeze film damper (DCSFD) [9]. Zhou et al. [10] studied on two types of floating ring squeeze film dampers, with single oil film and double layer of oil as FSFDS and FSFDS models. In these models, coupling effect between rotor, ball bearings and FSFDS/ FSFDD is considered. However, performance of these models are worse than DCSFD in preventing bistable and non- synchronous response, but better performance in controlling the transient process of the sudden balance response by increasing the support stiffness of the floating ring [10].

Also, Mevel Guyader [11, 12] simulated a system of a rigid rotor and two ball bearings and investigated its dynamic response. In this field, some researches have been carried out on some of the main ball bearing properties, such as radial clearance, waviness, radial load, damping factor, etc. In literature [13], variation of the bearing contact angle is investigated. In this model, the static ball deformations are obtained considering variation of the contact angle. It is reported that the main resonance regions for the rotor- bearing system shift to the lower speed ranges when the variation of contact angle is considered.

Harsha et al. [14] analyzed the effects of waviness in ball bearings on the rotor dynamic response. Liqin et al. [15] investigated the effects of the radial clearances and waviness on the dynamic behavior of a rotor- roller bearing system. Also, Xu Bai [16] have investigated the effects of clearance and waviness of races on the system dynamic response. In their research, the ball bearing model included the high - speed effects of ball centrifugal force and the gyroscopic moment.

In this research, the dynamic response of a rotor-ball bearing system with waviness and the squeeze film dampers is presented, in which the coupling effects between the rotor and the ball bearings and SFDs are considered, as in literature [17]. The direct numerical integration of the equations of motion of this system is applied and bifurcation graphs of the system's response are provided and investigated for a specific range of structural and operational parameters.

2. SYSTEM CHARACTERS

In this research, a flexible rotor system is modeled as a mass of m_D in the middle and two masses of m_j on either side of the model which are connected with a spring, K_R, which represents the stiffness of the shaft. The C_D is due to the effects of the aerodynamic damping exerted on the disc. The rotor is mounted on two identical bearings with the SFDs. The following assumptions have been considered in the equations:

- The rotor speed is constant.
- Damping force exerted on the disc due to the aerodynamic forces is viscous.
- Unbalance mass is defined as a point in the mid plane passing through the rotor center.
- The gyroscopic effects are neglected.
- Ball bearings are assumed to be short.
- Cavitation is modeled as π- film

Schematic model of the system and cross- sectional area of the ball bearing with SFD are illustrated in Figure 1.

A. Race Waviness

An important source of vibration in ball bearings is waviness. The geometric imperfections are often called waviness if its wavelength is much longer than Hertzian contact width. These are global sinusoidal- shaped imperfections on the bearing outer surface [14]. Figure 2 illustrates waviness in a ball bearing.

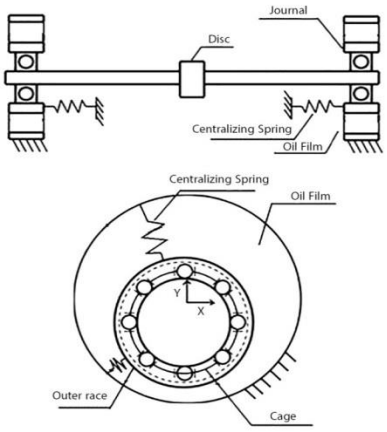

Figure 1. Schematic model of the system and cross-sectional area of the ball bearing with SFD

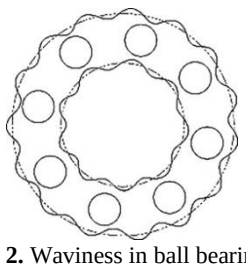

Figure 2. Waviness in ball bearing [14]

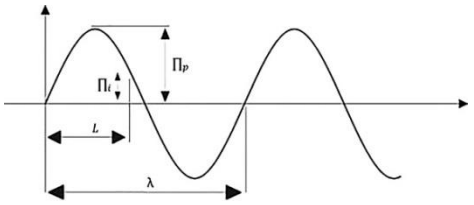

Figure 3. The relation between the wave parameters

Since waviness is assumed as a sinusoidal function, the wave amplitude at contact angle can be expressed as follows [14]:

$$\Pi_i = \Pi_0 + \Pi_p \sin(\frac{2\pi L_w}{\lambda}) \quad (1)$$

Wave parameters are illustrated in Figure 3. In this relation, Π_p and Π_0 are maximum and initial amplitude, respectively. Initial amplitude is constant clearance. L is inner race arc length at the contact angle:

$$L = r \times \theta_j \quad (2)$$

where, r is the inner race radius and θ_j indicates the angular position of j^{th} ball which is defined as follows [17]:

$$\theta_j = \omega \times \frac{r}{r+R} \times t + \frac{2\pi}{N_b}(j-1)\ ;\ \ j=1,2\ldots N_b \quad (3)$$

In which, N_b is the number of balls; t indicates time; r and R are inner and outer race radius, respectively. Since the wavelength is the race circumference divided by number of waves:

$$\lambda = \frac{2\pi r}{N_w} \quad (4)$$

N_w is number of wave lobes. As a result, the wave amplitude at the contact angle can be described as follows:

$$\Pi_i = \Pi_0 + \Pi_p \sin(N_w \theta_j) \quad (5)$$

B. Contact Forces

In ball bearings model, the contact forces between balls and races can be calculated by Hertzian theory. Since the inner race of ball bearing is fixed to the shaft and the outer race is fixed to the SFD. f_{Bx} and f_{By} are contact forces between balls and the outer race in x and y directions, respectively, which are created due to the clearance in the ball bearings. Waviness has been taken into consideration in these forces. The contact forces can be calculated as follows[11]:

$$F_{Bx} = \sum_{j=1}^{N_b} K_b[(x_j - x_O)\cos\theta_j + (y_j - y_O)\sin\theta_j - (R_0 + \Pi_i)]^{3/2} \ldots \\ .H[(x_j - x_O)\cos\theta_j + (y_j - y_O)\sin\theta_j - (R_0 + \Pi_i)]\cos\theta_j \quad (6a)$$

$$F_{By} = \sum_{j=1}^{N_b} K_b[(x_j - x_O)\cos\theta_j + (y_j - y_O)\sin\theta_j - (R_0 + \Pi_i)]^{3/2} \ldots \\ .H[(x_j - x_O)\cos\theta_j + (y_j - y_O)\sin\theta_j - (R_0 + \Pi_i)]\sin\theta_j \quad (6b)$$

where, R_0 is ball bearing radial clearance, K_b is contact stiffness related to the material and shape of the components and H is the Heaviside function in which, function value is equal to 1 if the term in brackets is positive, otherwise, the function is equal to zero.

C. Oil Film Forces

The oil pressure distribution P in short squeeze film damper is obtained by solving Reynolds equation for incompressible fluids [2]:

$$P(\theta,z) = \frac{6\mu}{C^2}(z^2 - \frac{L^2}{4})\frac{(\varepsilon\dot{\varphi}\sin\theta + \dot{\varepsilon}\cos\theta)}{(1+\varepsilon\cos\theta)^3} \quad (7)$$

So, the non-dimensional oil film forces along the x and y axes are as follows [2]:

$$f_{Sx} = -\frac{\mu R L^3}{C^2\sqrt{x_o^2 + y_o^2}}[x_o(\dot{\varepsilon}I_1 + \varepsilon\dot{\varphi}I_2) - y_o(\dot{\varepsilon}I_2 + \varepsilon\dot{\varphi}I_3)] \quad (8a)$$

$$f_{Sy} = -\frac{\mu R L^3}{C^2\sqrt{x_o^2 + y_o^2}}[y_o(\dot{\varepsilon}I_1 + \varepsilon\dot{\varphi}I_2) + x_o(\dot{\varepsilon}I_2 + \varepsilon\dot{\varphi}I_3)] \quad (8b)$$

where, f_{Sx} and f_{Sy} are oil-film forces in x and y directions, respectively. C is oil film thickness of SFD, μ is fluid viscosity, L is length of SFD, R is oil film radius, and also,ε is the non-dimensional eccentricity ratio of the journal:

$$\varepsilon = \frac{\sqrt{x_o^2 + y_o^2}}{C} \quad (9)$$

It should be mentioned that $\dot{\varepsilon}$ is time derivative of ε. Moreover, $\dot{\varphi}$ represents oil film angular velocity of the SFD which is derivative of the following equation with respect to t:

$$\tan\varphi = \frac{y_o}{x_o} \quad (10)$$

In addition, I_1, I_2 and I_3 are bearing integrals which can be obtained from Booker's integral table [18, 19].

D. Equations of Motion

According to Figure 1, only half of the system is considered because of symmetry, so, the differential equations of motion of the system are as follows:

$$m_D\ddot{x}_D + C_D\dot{x}_D + K_R(x_D - x_j) = m_D e_\mu \omega^2 \cos\omega t \quad (11a)$$

$$m_D\ddot{y}_D + C_D\dot{y}_D + K_R(y_D - y_j) = m_D e_\mu \omega^2 \sin\omega t \ldots \\ -m_D g \quad (11b)$$

$$m_j \ddot{x}_j + \frac{K_R}{2}\left(x_j - x_D\right) = -f_{Bx} \quad (11c)$$

$$m_j \ddot{y}_j + \frac{K_R}{2}\left(y_j - y_D\right) = -f_{By} - m_j g \quad (11d)$$

$$m_O \ddot{x}_O + \frac{K_a}{2} x_O = f_{Bx} + f_{Sx} \quad (11e)$$

$$m_O \ddot{y}_O + \frac{K_a}{2} y_O = f_{By} + f_{Sy} - m_O g \quad (11f)$$

where, (x_j, y_j), (x_D, y_D) and (x_O, y_O) are journal, disc and outer race displacement, respectively. m_D, m_j and m_O are lumped mass at the disc, journal and outer race position, respectively. C_D is viscous damping due to the aerodynamic effects, K_R is shaft stiffness, K_a is the centralizing springs' stiffness, e_μ is eccentricity of the middle disc of the rotor, g is gravity acceleration and ω is rotor angular speed. According to literature [11], the ball bearing parameters are:

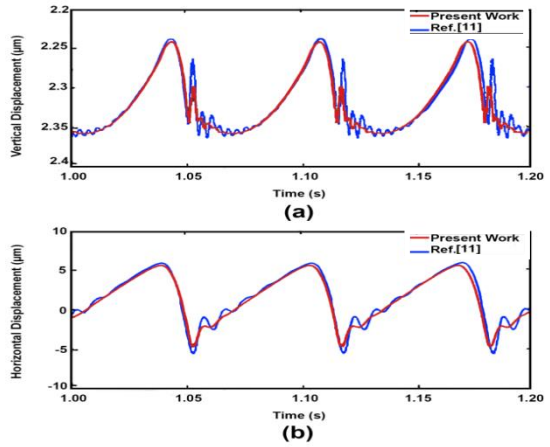

Figure4. (a) Time history for vertical y(t) motion; rotor speed n= 300 rpm for present work and literature [11]
(b) Time history for horizontal x(t) motion; rotor speed n= 300 rpm for present work and literature [11]

TABLE1. Ball bearing parameters

R_b	r_b	N_b	k_b	R_0
63.9 (mm)	40.1(mm)	8	13.34×10^9 ($N/m^{3/2}$)	20 (μm)

TABLE2. System parameters

M_D	C_D	K_R	e_μ	m_j	K_a
5(kg)	2.4867 (N.s/m)	1.2×10^6 (N/m)	4×10^{-5} (m)	0.5 (kg)	3×10^5 (N/m)

m_o	R	L	C	μ
0.1 (kg)	0.03 (m)	8.3×10^{-3} (m)	2×10^{-4} (m)	5×10^{-3} (Pa.s)

Waviness constant parameters are as follows [14]: $\prod_o$=2μm, $\prod_p$=3μm . Also, according to the iterature [17], other system's parameters are listed in Table 2. It should be noted that Runge-Kutta 4th-order method is used to solve the equations of motion of this system (Equation (11)).

3. RESULTS AND DISCUSSION

In order to verify the dynamic behavior of ball bearing, the results have been compared with the corresponding results in the literature [11]. The results are compared according to time history for vertical and horizontal motions which are illustrated in Figures. 4a and 4b, respectively. The results presented in these figures are in good agreement.

Moreover, validity of the simulation method of SFD has been investigated through the rotor response at the disc position in a certain speed range. Figure 5 shows the response of the rotor at the disc position along with x-direction, for the present work and literature [17]. The results presented in this figure are in good agreement.

In order to solve Equation (11) numerically, Matlab software has been utilized. The results are presented in bifurcation diagrams, time history for disc displacement and phase space graphs. Bifurcation diagrams show the system response for different angular velocities. With last 200 points obtained in Poincare maps, for different velocities, bifurcation diagrams are obtained. Poincare maps are obtained using the $x_D(T)$ versus of $\dot{x}_D(T)$ phase space graph sampling, at fixed time intervals equal to the system period ($T = 2\pi/\omega$). Phase space graphs show the disc displacement versus disc velocity along with x-direction in a certain speed. In this research, effects of key parameters of the SFD, namely the inner racemass of SFD (m_o), oil film thickness (C) and number of wave lobes of the ball bearings (N_w) on the system dynamic response are investigated. One of the main parameters of this system is waviness which is presented by a sinusoidal function.Since the accuracy in manufacturing the ball bearings depicted in the wave lobes number, the effects of this parameter are investigated in Figure 6.

In order to solve Equation (11) numerically, Matlab software has been utilized. The results are presented in bifurcation diagrams, time history for disc displacement and phase space graphs. Bifurcation diagrams show the system response for different angular velocities. With last 200 points obtained in Poincare maps, for different velocities, bifurcation diagrams are obtained. Poincare maps are obtained using the $x_D(T)$ versus of $\dot{x}_D(T)$ phase space graph sampling, at fixed time intervals equal to the system period ($T = 2\pi/\omega$). Phase space graphs show the disc displacement versus disc velocity along with x-direction in a certain speed.

In this research, effects of key parameters of the SFD, namely the inner racemass of SFD (m_o), oil film thickness (C) and number of wave lobes of the ball bearings (N_w) on the system dynamic response are investigated. One of the main parameters of this system is waviness which is presented by a sinusoidal function. Since the accuracy in manufacturing the ball bearings depicted in the wave lobes number, the effects of this parameter are investigated in Figure 6. By comparing Figures 6a, 6b, 6c, 6d and 6e it can be concluded that by increasing the number of wave lobes, which is due to inappropriate manufacturing, speed range with non-periodic behavior increases. In Figure 6a, periodic response can be seen, especially speed range of 1000 rad/s to 1400rad/s, as well as the range of 2000rad/s to 3000rad/s. It should be noted that in Figure 6a there are a few speeds with period-2, period-3 and non-periodic behaviors. However, by increasing the wave lobes number, one can see chaotic responses for most of rotational speeds and this procedure continues by increasing N_w.

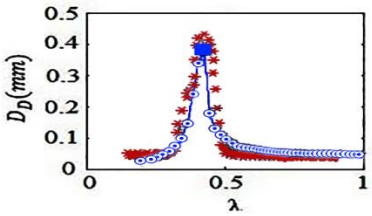

Figure 5. Rotor response at the disc position in present work (red stars) and referenc [17](blue circles)

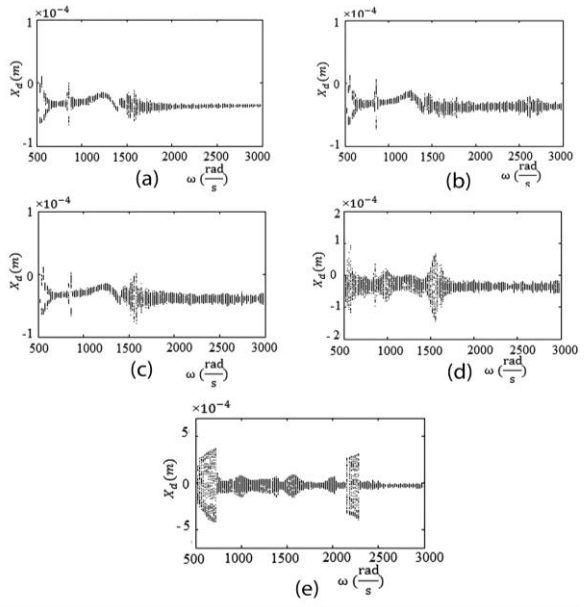

Figure 6. Bifurcation diagrams for $C_1=2\times10^{-4}$m, $m_o=0.1$kg, and (a) $N_w=0$, (b) $N_w=6$, (c) $N_w=8$, (d) $N_w=10$ and (e) $N_w=12$

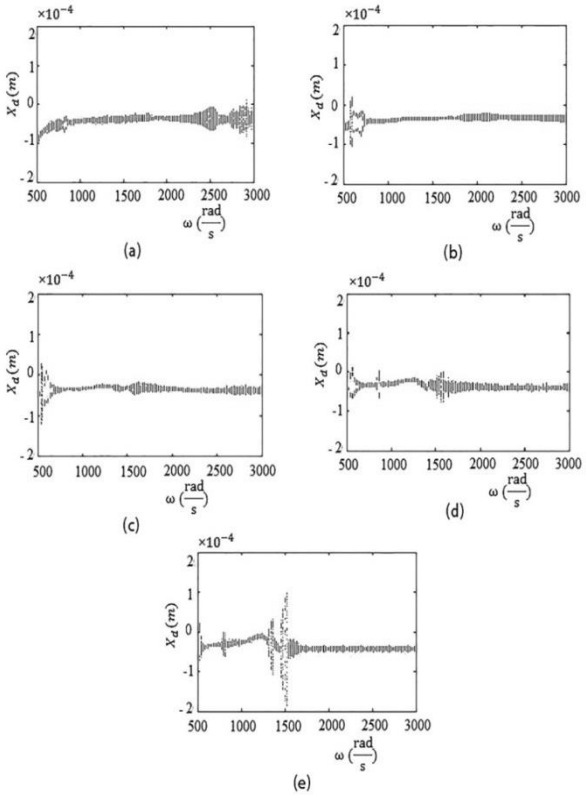

Figure 7. Bifurcation diagrams for $m_o=0.1$, $N_w=8$, and (a) $C=0.5\times10^{-4}$m, (b) $C=1\times10^{-4}$m, (c) $C=1.5\times10^{-4}$m, (d) $C=2\times10^{-4}$m, (e) $C=2.5\times10^{-4}$m

This results show the importance of the precision in manufacturing process of ball bearings. Moreover, it reveals the necessity of consideration the waviness in simulations.

Influence of oil film thickness of SFD is depicted in Figure 7. According to this figure, although the presence of oil film results in reduction the non-periodic and chaotic behaviors, but the oil film has an optimal thickness. It can be seen that non-periodic response of the system in Figure 7c is more than that of Figure 7a and 7b, which means that by increasing thickness, non-periodic and chaotic behavior decreases. This procedure has been reversed by increasing the oil film thickness. This means that for $C > 1.5\times10^{-4}$m, by increasing the oil film thickness, period-2, period-3, non-periodic and chaotic behavior can be observed, as in Figures 7c, 7d and 7e. For example, in the rotational speed of 1500 rad/s, chaotic response can be seen in Figure 7e, while in this speed, system response is periodic in Figure 7c.

The other main structural parameter of SFD which has been investigated is the inner race mass of SFD. According to Figure 8, by increasing the inner race mass of SFD, the non-periodic responses increase.

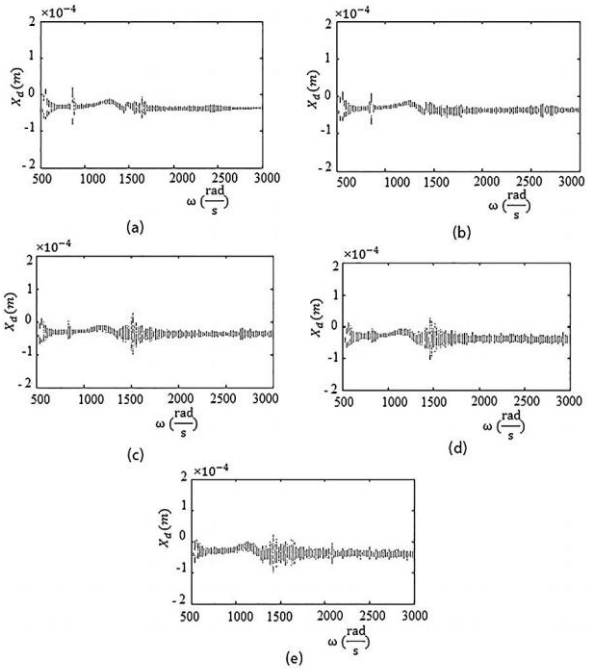

Figure 8. Bifurcation diagrams for $C=2\times10^{-4}$m, $N_w=6$, and (a) $m_o=0.05$kg, (b) $m_o=0.1$kg, (c) $m_o=0.15$kg, (d) $m_o=0.2$kg and (e) $m_o=0.25$kg

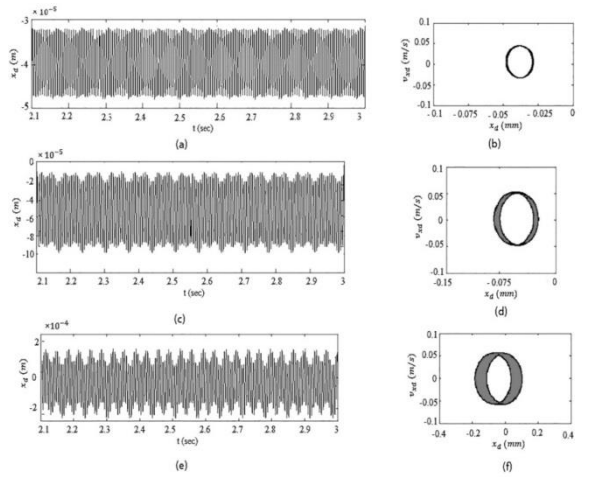

Figure 9. Time history for disc horizontal motion of the system with (a) $C=1.5\times10^{-4}$m, (c) $C=2\times10^{-4}$m and (e) $C=2.5\times10^{-4}$m, and also phase space diagrams for (b) $C=1.5\times10^{-4}$m, (d) $C=2\times10^{-4}$m and (f) $C=2.5\times10^{-4}$m

For example, in the speed range of 1400 rad/s to 1800 rad/s, non-periodic response of the system in Figure 8a and 8b, converts to chaotic response in Figure 8d and 8e. Moreover, periodic behavior of the system for the speed range of $\omega > 2000$rad/s in Figure 8a converts to the non-periodic behavior in Figure 8d and 8e. In Figure 9, changes in the system dynamic response for different C in a certain rotational speed are illustrated. This figure shows the time history for disc horizontal motion and phase space graphs for a certain speed of 1500 rad/s and different oil film thicknesses. It is demonstrated that as long as $C> 1.5\times10^{-4}$m, increasing the oil film thickness results in the system non-periodic and chaotic behavior, which can be seen in Figure 7, as well.

4. CONCLUSION

In this paper, effects of main parameters, namely the oil film thickness, C, inner race mass of SFD, m_o, and waviness, N_w, on system dynamic response of a rotor-ball bearings with waviness and the squeeze film dampers have been investigated. This research has been carried out over rotational speeds of 500rad/s to 3000rad/s which are the operational speed range for most of the rotational systems. The results show that by increasing the number of wave lobes, N_w, which is due to inappropriate manufacturing, non- periodic and chaotic behavior increases. This procedure is obvious in whole the speed range, whether in low speeds, in which by increasing Nw, the periodic and period-2 responses convert to chaotic responses, or in high speeds, in which the periodic behavior converts to non-periodic behavior, as N_w increases.

This result reveals the importance of manufacturing accuracy. Moreover, as long as $C< 1.5\times10^{-4}$m, by increasing the oil film thickness, unwanted vibrations and non-periodic behavior of the system have been reduced, On the other hand, when $C> 1.5\times10^{-4}$m, increasing the outer oil film thickness results in the increasing chaotic and non-periodic responses. This result shows that although the presence of oil film results in reduction the non-periodic and chaotic behaviors, but the oil film has an optimal thickness. In addition, with increasing m_o, the disc displacement amplitude increases. This result reveals the importance of utilizing light materials in manufacturing the squeeze film dampers. At the end, it should be mentioned that chaos and non-periodic behavior, in addition to noise and vibration, cause unwanted stresses and fatigue failures which reveal the importance of these results on systems design and operation.

5. REFERENCES

1. Rezvani, M. and Hahn, E., "Floating ring squeeze film damper: Theoretical analysis", ***Tribology International***, Vol. 33, No. 3, (2000), 249-258.
2. Inayat-Hussain, J.I., "Bifurcations of a flexible rotor response in squeeze-film dampers without centering springs", ***Chaos, Solitons & Fractals***, Vol. 24, No. 2, (2005), 583-596.

3. Inayat-Hussain, J.I., "Bifurcations in the response of a flexible rotor in squeeze-film dampers with retainer springs", ***Chaos, Solitons & Fractals***, Vol. 39, No. 2, (2009), 519-532.
4. Inayat-Hussain, J., Kanki, H. and Mureithi, N., "On the bifurcations of a rigid rotor response in squeeze-film dampers", ***Journal of Fluids and Structures***, Vol. 17, No. 3, (2003), 433-459.
5. Vance, J., "Effect of fluid inertia on the performance of squeeze film damper supported rotors", ***Journal of Engineering for Gas Turbines and Power***, Vol. 110, No., (1988), 51-57.
6. Weiyang, Q., Jinfu, Z. and Xingmin, R., "Response and bifurcation of rotor with squeeze film damper on elastic support", (2009).
7. Jacobs. W., Boonen. R., Sas. P. and Moens. D., "The influence of the lubricant film on stiffness and damping charactristics of a deep groove ball bearing", ***Mechanical Systems and Signal Processing***, Vol. 42, (2014), 335- 350.
8. Zhao, J. and Hahn, E., "Eccentric operation and blade-loss simulation of a rigid rotor supported by an improved squeeze film damper", ***Journal of Tribology***, Vol. 117, No. 3, (1995), 490-497.
9. Zhou, H.L., Luo, G.H., Chen, G. and Tian, H.T., "Two dynamic models of dual clearance squeeze film damper and their verification", ***Tribology International***, Vol. 66, (2013), 187-193.
10. Zhou, H.-l., Feng, G.-q., Luo, G.-h., Ai, Y.-t. and Sun, D., "The dynamic characteristics of a rotor supported on ball bearings with different floating ring squeeze film dampers", ***Mechanism and Machine Theory***, Vol. 80, (2014), 200-213.
11. Mevel, B. and Guyader, J., "Routes to chaos in ball bearings", ***Journal of Sound and Vibration***, Vol. 162, No. 3, (1993), 471-487.
12. Mevel, B. and Guyader, J.-L., "Experiments on routes to chaos in ball bearings", ***Journal of Sound and Vibration***, Vol. 318, No. 3, (2008), 549-564.
13. Zhang, X., Han, Q., Peng, Z. and Chu, F., "A new nonlinear dynamic model of the rotor-bearing system considering preload and varying contact angle of the bearing", ***Communications in Nonlinear Science and Numerical Simulation***, Vol. 22, No. 1, (2015), 821-841.
14. Harsha, S., Sandeep, K. and Prakash, R., "The effect of speed of balanced rotor on nonlinear vibrations associated with ball bearings", ***International Journal of Mechanical Sciences***, Vol. 45, No. 4, (2003), 725-740.
15. Liqin, W., Li, C., Dezhi, Z. and Le, G., "Nonlinear dynamics behaviors of a rotor roller bearing system with radial clearances and waviness considered", ***Chinese Journal of Aeronautics***, Vol. 21, No. 1, (2008), 86-96.
16. Changqing, B. and Qingyu, X., "Dynamic model of ball bearings with internal clearance and waviness", ***Journal of Sound and Vibration***, Vol. 294, No. 1, (2006), 23-48.
17. Zhou, H.-l., Luo, G.-h., Chen, G. and Wang, F., "Analysis of the nonlinear dynamic response of a rotor supported on ball bearings with floating-ring squeeze film dampers", ***Mechanism and Machine Theory***, Vol. 59, (2013), 65-77.
18. Booker, J., "A table of the journal-bearing integral", ***Journal of Fluids Engineering***, Vol. 87, No. 2, (1965), 533-535.
19. Zhu, C., Robb, D. and Ewins, D., "Analysis of the multiple-solution response of a flexible rotor supported on non-linear squeeze film dampers", ***Journal of Sound and Vibration***, Vol. 252, No. 3, (2002), 389-408.

Dynamic Analysis of a Rotor Supported on Ball Bearings with Waviness and Centralizing Springs and Squeeze Film Dampers

S. Modaresahmadi[a], M. Ghazavi [a], M. Sheikhzad Saravani [b]

[a]*Department of Mechanical Engineering, TarbiatModares University, Tehran, Iran*
[b]*Department of Mechanical Engineering, University of Wollongong,Wollongong,Australia*

P A P E R I N F O

Paper history:
Received 13 October 2014
Received in revised form 10 August 2015
Accepted 03 September 2015

Keywords:
Squeeze-film Damper
Waviness
Ball Bearing
Bifurcation

چکیده

دمپرهای فیلم فشار (SFD) معمولا در ماشین‌های دوار با سرعت بالا استفاده می‌شوند تا رفتار نامتناوب سیستم را با ایجاد میرایی اضافی، کاهش دهند. چندین پارامتر ساختاری وجود دارد که در طراحی این نوع سیستم‌ها از اهمیت ویژه‌ای برخوردارند، از جمله این پارامترها می‌توان به ضخامت فیلم روغن و جرم حلقه‌ی داخلی SFD اشاره نمود. بعلاوه، پارامتر بسیار مهم دیگری نیز وجود دارد که در مراحل ساخت و تولید یاتاقان بروز می‌کند، به نام اعوجاج. نواقص و عیوب هندسی را غالبا اعوجاج می‌نامند، اگر طول موج آن بسیار بزرگ‌تر از عرض تماس Hertzian باشد. این عامل، منبعی قابل ملاحظه در تولید ارتعاشات در یاتاقان‌های غلتشی می‌باشد. در این مقاله، سیستمی دارای روتور انعطاف پذیر و دو یاتاقان غلتشی معوج به همراه دمپرهای فیلم فشار و فنرهای مرکز گرا مدل‌سازی شده‌اند و معادلات حرکت آن به کمک روش انتگرال عددی حل شده و پاسخ دینامیکی سیستم بدست آمده است. نتایج بدست آمده نشان می‌دهند که با افزایش تعداد موج‌های مربوط به اعوجاج که حاصل از فرایند ساخت نامناسب می‌باشد، رفتار نامتناوب و بعضاً آشوبناک سیستم افزایش می‌یابد. این مطلب گویای اهمیت دقت در ساخت و لزوم در نظر گرفتن این عامل در شبیه‌سازی سیستم می‌باشد. بعلاوه، با تغییر ضخامت فیلم روغن، مشخص می‌گردد که یک مقدار بهینه برای این پارامتر وجود دارد که حداکثر میرایی را فراهم می‌آورد. همچنین با افزایش جرم حلقه‌ی داخلی SFD، دامنه‌ی جابجایی دیسک افزایش می‌یابد. این مطلب اهمیت بکارگیری مواد سبک‌تر در ساخت دمپرهای فیلم فشار را نشان می‌دهد.

***doi**: 10.5829/idosi.ije.2014.28.09c.13*